Puskas, R. S., Manley, N. R., Wallace, D. M., & Berger, S. L. (1982) *Biochemistry 21*, 4602-4608.
Reid, T. W., & Wilson, I. B. (1971) *Biochemistry 10*, 380-387.
Rollison, C. L. (1973) in *Comprehensive Inorganic Chemistry* (Bailar, J. C., Jr., Emeléus, H. J., Nyholm, R., & Trotman-Dickenson, A. F., Eds.) Vol. 3, pp 738-768, Pergamon Press, New York.
Rosen, O. M., Herrera, R., Olowe, Y., Petruzzelli, L. M., & Cobb, M. H. (1983) *Proc. Natl. Acad. Sci. U.S.A. 80*, 3237-3240.
Sefton, B. M., Hunter, T., Nigg, E. A., Singer, S. J., & Walter, G. (1982) *Cold Spring Harbor Symp. Quant. Biol. 46*, 939-951.
Smith, J. B. (1983) *Proc. Natl. Acad. Sci. U.S.A. 80*, 6162-6166.
Sowadski, J. M., Handschumacher, M. D., Murthy, H. M. K., Foster, B. A., & Wycoff, H. M. (1985) *J. Mol. Biol. 186*, 417-433.
Sparks, J. W., & Brautigan, D. L. (1985) *J. Biol. Chem. 260*, 2042-2045.
Sparks, J. W., & Brautigan, D. L. (1986) *Int. J. Biochem. 18*, 497-504.
Spence, J. T., & Lee, J. Y. (1965) *Inorg. Chem. 4*, 385-388.
Swarup, G., Cohen, S., & Garbers, D. L. (1981) *J. Biol. Chem. 256*, 8197-8201.
Swarup, G., Cohen, S., & Garbers, D. L. (1982a) *Biochem. Biophys. Res. Commun. 107*, 1104-1109.
Swarup, G., Speeg, K. V., Jr., Cohen, S., & Garbers, D. L. (1982b) *J. Biol. Chem. 257*, 7298-7301.
Tamura, S., Brown, T. A., Whipple, J. H., Fujita-Yamaguchi, Y., Dubler, R. E., Cheng, K., & Larner, J. (1984) *J. Biol. Chem. 259*, 6650-6658.
Tracey, A. S., & Gresser, M. J. (1986) *Proc. Natl. Acad. Sci. U.S.A. 83*, 609-613.
Tsuboi, K. K., & Huson, P. B. (1955) *Arch. Biochem. Biophys. 55*, 191-205.
Uehara, K., Fujimoto, S., & Tanigchi, T. (1974) *J. Biochem. (Tokyo) 75*, 627-638.
Ushiro, H., & Cohen, S. (1980) *J. Biol. Chem. 255*, 8363-8365.
Van Etten, R. L., Waymock, P. P., & Rehkop, D. M. (1974) *J. Am. Chem. Soc. 96*, 6782-6785.
Westheimer, F. H. (1949) *Chem. Rev. 45*, 419-451.
Wiberg, K. B. (1965) *Oxidations in Organic Chemistry*, Part A, pp 69-184, Academic Press, New York.
Wiberg, K. B., & Mukherjee, S. K. (1974a) *J. Am. Chem. Soc. 96*, 1884-1889.
Wiberg, K. B., & Mukherjee, S. L. (1974b) *J. Am. Chem. Soc. 96*, 6647-6651.
Williams, A., & Naylor, R. A. (1971) *J. Chem. Soc. B*, 1973-1979.

Isotope Partitioning for NAD-Malic Enzyme from *Ascaris suum* Confirms a Steady-State Random Kinetic Mechanism†

Cheau-Yun Chen, Ben G. Harris, and Paul F. Cook*
Department of Biochemistry, Texas College of Osteopathic Medicine/North Texas State University, Denton, Texas 76203
Received July 10, 1987; Revised Manuscript Received September 11, 1987

ABSTRACT: Isotope partitioning studies beginning with E·[^{14}C]NAD, E·[^{14}C]malate, E·[^{14}C]NAD·Mg^{2+}, and E·Mg·[^{14}C]malate suggest a steady-state random mechanism for the NAD-malic enzyme. Isotope trapping beginning with E·[^{14}C]NAD and with varying concentrations of Mg^{2+} and malate in the chase solution indicates that Mg^{2+} is added in rapid equilibrium and must be added prior to malate for productive ternary complex formation. Equal percentage trapping from E·[^{14}C]NAD·Mg and E·Mg·[^{14}C]malate indicates the mechanism is steady-state random with equal off-rates for NAD and malate from E·NAD·Mg·malate. The off-rates for both do not change significantly in the ternary E·Mg·malate and E·NAD·Mg complexes, nor does the off-rate change for NAD from E·NAD. No trapping of malate was obtained from E·[^{14}C]malate, suggesting that this complex is nonproductive. A quantitative analysis of the data allows an estimation of values for a number of the rate constants along the reaction pathway.

The NAD-malic enzyme from *Ascaris suum* is proposed to have a steady-state random mechanism in the direction of oxidative decarboxylation of malate. The mechanism is based on initial velocity studies varying substrate and metal ion concentrations over a wide range (Park et al., 1984), determination of enzyme-reactant dissociation constants (Kiick et al., 1984), and deuterium isotope effects (Kiick et al., 1986). Further, it has been proposed that two of the transitory enzyme-substrate complexes, E·malate and E·NAD·malate, are nonproductive.

Recently, studies on the malic enzyme (Kiick et al., 1986) have shown small deuterium isotope effects of 1.45 on V/K_{malate}, V/K_{NAD}, and V_{max}. This suggests that hydride transfer may not be the primary rate-limiting step. $^{D}(V/K_{malate})$ and $^{D}(V/K_{NAD})$ remained constant over the pH range of 5-10, but $^{D}V_{max}$ decreases to a value of 1 at low pH values. The change in $^{D}V_{max}$ with pH gave a pK about 4.9 in agreement with that obtained for the pH dependence of V_{max} and suggests that NADH release limits the rate of the reaction partially at

† This work was supported by National Institutes of Health Grants AI 24155 (B.G.H.) and GM 36799 (P.F.C.), Robert A. Welch Foundation Grants B-997 (B.G.H.) and B-1031 (P.F.C.), World Health Organization Grant OCT-83011 (B.G.H.), and National Institutes of Health Biomedical Research Grants Program Grant BRSG S07 RR 07195-07 (P.F.C.). P.F.C. is the recipient of NIH Research Career Development Award AM 01155.

0006-2960/88/0427-0212$01.50/0

neutral pH and becomes completely rate determining at low pH. This is in agreement with the proposal from inhibition studies (Kiick et al., 1986) that the release of NADH from E·NADH completely limits the overall reaction at low pH. As a result, the equal isotope effects on $^{D}(V/K_{NAD})$ and $^{D}(V/K_{malate})$ suggest a steady-state random mechanism in which the off-rates for NAD and malate from the central complex are equal.

In the present study, isotope partitioning is used to test the proposed steady-state random mechanism and to determine values for the reactant off-rates as compared to the net rate for the catalytic steps. Results confirm the steady-state mechanism.

Materials and Methods

Chemicals and Enzyme. Mitochondrial NAD–malic enzyme from *Ascaris suum* was purified according to the procedure of Allen and Harris (1981). Enzyme was homogeneous by the criterion of SDS[1]–polyacrylamide gel electrophoresis run according to the method of O'Farrel (1975) as modified by Atkins et al. (1975). Enzyme had a final specific activity of 34 units/mg assayed in the direction of oxidative decarboxylation with 100 mM Hepes, pH 7.5, 1.0 mM DTT, 153.4 mM malate (28 mM uncomplexed), 13.5 mM NAD (2 mM uncomplexed), and 249 mM $MgSO_4$ (112 mM when corrected for Mg·malate and Mg·NAD chelate complexes). The stock malic enzyme solution was tested for malate dehydrogenase contamination with an assay containing 100 mM Hepes, pH 7.5, 0.2 mM NADH, 0.5 mM oxalacetate, 2 mM EDTA, and 1 mM DTT. A contamination of less than or equal to 0.1% of the malic enzyme oxidative decarboxylation activity was found. Protein concentration was determined by the method of Bradford (1976) with bovine serum albumin as a standard. Purified *A. suum* malic enzyme was stored at −20 °C in a storage buffer containing 10 mM Hepes (pH 7.5), 10 mM DTT, 1 mM EDTA, and 20% glycerol.

[*carbonyl*-^{14}C]NAD (56 mCi/mmol) and L-[U-^{14}C]malic acid (46 mCi/mmol) were obtained from Amersham. The NAD and NADP were purchased from Boehringer-Mannheim. L-Malate and DTT were from Sigma. All other reagents and chemicals were obtained from commercially available sources and were of the highest purity available.

Substrate Concentration Calibration. The L-malate concentration was determined enzymatically with 2 units of chicken liver malic enzyme, 1 mM NADP, 2 mM $MgSO_4$, and 100 mM Taps (pH 9.0) as described by Cook et al. (1980). The concentration of NAD was determined spectrophotometrically with an extinction coefficient of 17 800 M^{-1} cm^{-1} at 259 nm.

Isotope Partitioning Experiments. Isotope partitioning studies were performed according the the method of Rose et al. (1974). Isotope partitioning studies at 25 °C using five enzyme–substrate complexes (E·NAD, E·NAD·Mg, E·malate, E·Mg·malate, and E·NAD·malate) were carried out.

The concentrations of the enzyme–substrate complexes present in the pulse solution were calculated according to the dissociation constant of the enzyme–substrate complex. For the binary enzyme–substrate complexes, the concentration was calculated according to

$$[EA] = [E_t]/(1 + K_{iA}/[A_f]) \quad (1)$$

where $[E_t]$ is the total enzyme concentration added to the pulse solution, $[A_f]$ is the uncomplexed substrate concentration, [EA] is the final desired concentration of binary enzyme–substrate complex, and K_{iA} is the equilibrium constant for dissociation of the enzyme–substrate complex ($K_{iA} = [E_f][A_f]/[EA]$). The total concentration of substrate equals the sum of $[A_f]$ and [EA].

For the ternary enzyme–substrate complexes, the concentration was calculated according to

$$[EAB] = [E_t]/\{1 + (K_{iA}/[A_f])(K_{IB}/K_{iB}) + K_{IB}/[B_f] + (K_{iA}/[A_f])(K_{IB}/[B_f])\} \quad (2)$$

where $[E_t]$, K_{iA}, and $[A_f]$ have the same definition as above, K_{iB} is the equilibrium constant for dissociation of the enzyme–substrate complex EB ($K_{iB} = [E_f][B_f]/[EB]$), K_{IB} is the equilibrium constant for dissociation of B from the EAB ternary complex ($K_{IB} = [B_f][EA]/[EAB]$), and [EAB] is the desired concentration of ternary enzyme–substrate complex. The total concentration of substrates A and B to be added was calculated according to

$$[A_t] = [A_f] + [AB] + [EA] + [EAB] \quad (3)$$

$$[B_t] = [B_f] + [AB] + [EB] + [EAB] \quad (4)$$

where [AB] is the concentration of AB complex ($[AB] = [A_f][B_f]/K_{AB}$) and K_{AB} is the dissociation constant of a chelate complex between two substrates, A and B, and is applicable when A or B is Mg. [EA] and [EB] are the concentrations of binary enzyme–substrate complexes, and [EAB] has the same definition as above. Dissociation constants used in the above calculations are as follows: $K_{i\,NAD}$, 80 μM (Park et al., 1984); $K_{i\,Mg}$, 14 mM; $K_{i\,(E\cdot NAD)Mg}$, 29.3 mM; $K_{i\,malate}$, 20 mM; $K_{I\,malate}$, 1.6 mM; $K'_{I\,malate}$, 35 mM (Kiick et al., 1984). $K_{I\,malate}$ is the dissociation constant for malate from E·Mg·malate. $K'_{I\,malate}$ is the dissociation constant for malate from E·NAD·malate. The dissociation constant for chelate complexes are as follows: $K_{Mg\cdot NAD}$, 19.5 mM; $K_{Mg\cdot malate}$, 25.1 mM (Martell & Smith, 1979).

Isotope trapping with [^{14}C]NAD was investigated in the binary complex E·NAD and ternary complexes E·NAD·Mg and E·NAD·malate. In the former case, a 0.05-mL pulse solution contained 325 μg of malic enzyme (5 nmol of binding sites based on a tetrameric M_r of 265 000) and 0.88 mM [^{14}C]NAD (7000 cpm/nmol), giving a final concentration of E·[^{14}C]NAD equal to 0.091 mM. This solution was added to a vigorously stirring 5.0-mL chase solution. Both pulse and chase solutions were incubated at 25 °C for 10 min prior to addition. The chase solution contained sufficient unlabeled NAD for a 400-fold dilution of labeled NAD (once added to a chase), a varied concentration of uncomplexed malate from 1 to 10 mM, 1 mM uncomplexed Mg^{2+} as $MgSO_4$, 1 mM DTT, and 100 mM Hepes, pH 7.5. This experiment was then repeated at 17 and 50 mM uncomplexed Mg^{2+} concentrations. The reaction was terminated 2 s after adding the pulse to the chase solution by the addition of potassium oxalate at pH 7.0. An amount of potassium oxalate was added that would quench the reaction by instantaneously chelating 99% of the Mg^{2+} and was calculated according to the dissociation constant of 1.7 mM for Mg·oxalate (Martell & Smith, 1979). After the pH was adjusted to 10 with 1 M LiOH, a 1.0-mL aliquot of the quenched reaction mixture was loaded onto an 8-mL AGMP-1 column to isolate the [^{14}C]NADH according to the method of Viola et al. (1979). The unreacted [^{14}C]NAD was eluted with 0.4 M LiCl (pH 10), while the [^{14}C]NADH produced from the reaction was eluted with 1 M LiCl (pH 10). A 1.0-mL aliquot of the NADH fraction pool was mixed with

[1] Abbreviations: Hepes, *N*-(2-hydroxyethyl)piperazine-*N*′-2-ethanesulfonic acid; TAPS, 3-[[tris(hydroxymethyl)methyl]amino]propanesulfonic acid; DTT, dithiothreitol; EDTA, ethylenediaminetetraacetic acid; SDS, sodium dodecyl sulfate.

9 mL of Aquasol scintillation cocktail and counted for ^{14}C to determine the amount of [^{14}C]NADH produced. An individual control was run for each malate concentration in which the same amount of [^{14}C]NAD was present in the 5-mL chase solution before the addition of enzyme. The control value was then subtracted from the experimental value to give the actual amount of [^{14}C]NAD trapped.

A malate dehydrogenase control was also carried out with 1 mM EDTA in both pulse and chase solution. The chase solutions contained no $MgSO_4$, 3.5 mM NAD, 7.5 mM malate, 1 mM DTT, and 100 mM Hepes, pH 7.5. The resulting amount of [^{14}C]NADH produced over control was negligible.

Analysis of isotope trapping in the ternary E·NAD·Mg complex was carried out similarly to the experiment described above. The pulse solutions consisted of the same amount of enzyme, 93.7 mM $MgSO_4$ (90 mM, when corrected for chelate complex), and 4.5 mM [^{14}C]NAD (4500 cpm/nmol) (0.8 mM, when corrected for chelate complex) giving a final concentration of E·[^{14}C]NAD·Mg equal to 0.069 mM. The chase solution contained 137.9 mM NAD (sufficient for a 3000-fold dilution of labeled NAD once added to the chase solution), 100 mM uncomplexed $MgSO_4$, and varying levels of uncomplexed malate from 1 to 10 mM. The pulse solution was added to a vigorously stirring chase solution, and the reaction was quenched after 5 s as described above. The isolation of [^{14}C]NADH was performed on a Bio-Rad model HPLC using a C_{18} reverse-phase preparative column instead of the AGMP-1 column. An internal standard of NADH at a final concentration of 0.4 mM was included in all of the solutions. A 0.4-mL aliquot of the solution was applied to the HPLC according to the method of Miksic and Brown (1977). The chromatography was developed with a linear gradient from 0 to 24% over 180 min at a flow rate of 2 mL/min. The starting solution was 10 mM KH_2PO_4 at pH 7, and the second solution was methanol/H_2O (60:40 v/v). The elution profile was determined by monitoring the absorbance at 260 and 340 nm. The retention time of NAD was 90 min, while the retention time of NADH was 120 min. A 1-mL aliquot of the pooled [^{14}C]NADH was counted and analyzed as described above.

Isotope partitioning of E·NAD·malate was also performed as described above except that 5 mM [^{14}C]NAD, 200 mM malate (giving a final E·[^{14}C]NAD·malate concentration equal to 0.083 mM), and 10 mM EDTA were included in the pulse solution. The [^{14}C]NADH produced was isolated via HPLC by reverse-phase preparative column chromatography on C_{18} as described above.

Isotope partitioning experiments with [^{14}C]malate in both the binary E·malate and ternary E·Mg·malate complexes were carried out as above. For the E·Mg·malate reaction, each 0.05-mL pulse solution contained 325 g of malic enzyme (5 nmol of binding sites), 65.7 mM [^{14}C]malate (800 cpm/nmol), and 65.7 mM $MgSO_4$ (which gave a final concentration of E·Mg·malate equal to 0.084 mM). For the E·malate reaction, 30.5 mM [^{14}C]malate (800 cpm/nmol) (which gave a final conentration of E·[^{14}C]malate equal to 0.06 mM) and 10 mM EDTA were included in each of the pulse solutions. For the E·Mg·malate reaction, the 5-mL chase solution contained sufficient unlabeled malate for a 833-fold dilution of labeled malate once added to the chase, 105.2 mM uncomplexed $MgSO_4$, 100 mM Hepes (pH 7.5), 1 mM DTT, and varying levels of uncomplexed NAD from 0.002 to 0.5 mM. For the E·malate reaction, sufficient unlabeled malate for a 1500-fold dilution of labeled malate once added to the chase, 50 mM uncomplexed $MgSO_4$, and 0.5 mM uncomplexed NAD were included in the chase. The reaction was stopped after 5 s by the rapid addition of 0.36 mL of 10 N KOH. The quenched solution was centrifuged, and a 3.6-mL aliquot of the supernatant was back-titrated to pH 9.0. The [^{14}C]pyruvate produced was then converted to [^{14}C]alanine by the addition of 100 mM Taps (pH 9.0), 25 mM $(NH_4)_2SO_4$, 1 mM NADH, and 50 units of alanine dehydrogenase. The completion of conversion was determined by monitoring the depletion of NADH in a 0.1-cm path-length cuvette at 340 nm. After 1 h, the reaction was stopped by addition of 0.3 mL of concentrated H_2SO_4 which adjusted the pH to below 1. The entire resulting reaction mixture was added to an 8-mL Dowex 50W-X12 column. The unreacted [^{14}C]malate was eluted with 50 mL of H_2O followed by elution of [^{14}C]alanine with 4 N pyridine. The pooled alanine fractions were counted to determine the [^{14}C]pyruvate produced. Individual controls were run as described for the NAD trapping experiments to correct for the amount of [^{14}C]pyruvate produced from the free [^{14}C]malate and enzyme.

Data Analysis. Results of isotope partitioning were plotted graphically as double-reciprocal plots of P^* vs the concentration of reactant varied in the chase solution. Data were fitted with the appropriate rate equation and FORTRAN programs developed by Cleland (1979). Data for isotope trapping of (E·Mg·[^{14}C]malate; E·[^{14}C]NAD·Mg) ternary complexes were fitted with eq 5, where P^* is the observed

$$P^* = \frac{P^*_{max}[A]}{K' + [A]} \quad (5)$$

amount of trapped product at a given concentration of A, the substrate varied in the chase. K' is the K_m for A in the trapping experiment and is the concentration of A that gives one-half P^*_{max}, P^*_{max} is the maximum amount of P^* formed at infinite concentration of A, and A is NAD or malate for E·Mg·malate and E·NAD·Mg trapping experiments, respectively. Data for isotope trapping from the (E·[^{14}C]NAD) binary complex were first analyzed graphically. The data obtained at each Mg^{2+} concentration with varying malate were initially fitted with eq 5. Data conformed to a rapid equilibrium ordered addition of one Mg prior to malate, and all data were then fitted with eq 6, where B and C are Mg^{2+} and malate, K_C' is the K_m for

$$P^* = \frac{P^*_{max}[B][C]}{K_{iB}'K_C' + K_C'[B] + [B][C]} \quad (6)$$

malate in the trapping experiments, K_{iB}' is the K_i for Mg^{2+} in the trapping reaction obtained under conditions in which malate is limiting, and P^*_{max} has the same definition as above.

THEORY

The fundamental theory of isotope partitioning experiments is that the isotope-labeled substrate in the enzyme–substrate complex can partition in different directions. Within the first turnover, the amount of product being trapped is determined by the partition ratios for substrate dissociation and product formation. The experimental design and basic theory have been well described (Rose et al., 1974; Cleland, 1975; Rose, 1980).

The above were developed for a bireactant enzyme reaction. For an ordered terreactant reaction, the rate equation has been derived for a specific case by Meek et al. (1982). The scheme in eq 7 can be used to analyze isotope partitioning data for an ordered terreactant enzyme.

The radiolabeled substrate A* in the EA* complex can dissociate from any of the three transitory complexes EA*, EA*B, and EA*BC or can be trapped as the radiolabeled

$$\begin{array}{ccccccc} EA^* & \underset{k_4}{\overset{k_3B}{\rightleftharpoons}} & EA^*B & \underset{k_6}{\overset{k_5C}{\rightleftharpoons}} & EA^*BC & \xrightarrow{k_{15}} & E + P^* \\ \downarrow{\scriptstyle k_2} & & \downarrow{\scriptstyle k_9} & & \downarrow{\scriptstyle k_8} & & \\ E + A^* & & EB + A^* & & EBC + A^* & & \end{array} \quad (7)$$

product P*. The amount of P* being formed from EA* can be determined according to (Cleland, 1975)

$$\frac{[EA_0^*]}{P^*} = \left(1 + \frac{k_2}{k_3'}\right)\left(1 + \frac{k_9}{k_5'}\right)\left(\frac{[EA_0^*]}{P^*_{max}}\right) = \left(1 + \frac{K_B'}{[B]} + \frac{K_C'}{[C]} + \frac{K_{iB}'K_C'}{[BC]}\right)\left(\frac{[EA_0^*]}{P^*_{max}}\right) \quad (8)$$

where $[EA^*]/P^*_{max} = (1 + k_{15}/k_8)$, k_3' and k_5' are net rate constants for P* production beginning with EA* and EA*B, respectively, and the remaining parameters are

$$K_B' = k_2/k_3 \quad (9)$$

$$K_C' = k_9(k_6 + k_8 + k_{15})/[k_5(k_8 + k_{15})] \quad (10)$$

$$K_{iB}' = k_2(k_4 + k_9)/(k_3k_9) \quad (11)$$

In the above equations, K_B' and K_C' are the K_m values for B and C in the isotope trapping reaction, i.e., obtained at infinite concentrations of C and B, respectively, while K_{iB}' is the K_i for B in the trapping reaction obtained under conditions in which C is limiting. Under conditions where B and C are saturating, the ratio of the rate constant for A dissociating from the central complex EA*BC (k_8) to the rate constant for production of P* (k_{15}) can be calculated from the ratio of $[EA_0^*]/P^*_{max}$ as shown above. Under conditions where B is saturating and C is limiting, a range for the ratio of the rate constant for A dissociating from EA*B (k_9) to the rate constant for production of P* (k_{15} or $V/[E_t]$) can be obtained as

$$\frac{VK_C'}{[E_t]K_C} = \frac{k_9k_{15}(k_6 + k_8 + k_{15})}{(k_8 + k_{15})(k_6 + k_{15})} = k_9/\left[1 + \frac{k_6k_8}{k_{15}(k_6 + k_8 + k_{15})}\right] \quad (12)$$

$$\frac{k_9}{V/[E_t]} = \frac{K_C'}{K_C}\left\{1 + \left(\frac{[EA^*]}{P^*_{max}} - 1\right)\frac{k_6}{k_6 + k_8 + k_{15}}\right\} \quad (13)$$

Thus

$$\frac{K_C'}{K_C} \leq \frac{k_9}{V/[E_t]} \leq \frac{K_C'}{K_C}\frac{[EA^*]}{P^*_{max}} \quad (14)$$

where K_C is the Michaelis constant for C from initial velocity studies. The upper limit of this ratio is observed if k_6 is much greater than $(k_8 + k_{15})$, that is, if C is in rapid equilibrium with EA*BC. The lower limit of this ratio is observed if k_{15} is much greater than k_8, that is, if A is very sticky in the EA*BC complex. Under conditions where B and C are limiting, the ratio of the off-rate of substrate from the binary complex to the off-rate of substrate from the ternary complex can be obtained as

$$\frac{K_{iB}' - K_B'}{K_{iB}} = \frac{k_2}{k_9} \quad (15)$$

Thus, limits on the ratio of the rate constant for A* dissociating from EA* (k_2) to that trapped as P^*_{max} (k_{15} or $V/[E_t]$) can be determined according to eq 16, where K_{iB} is the dissociation

$$\frac{K_C'}{K_C}\frac{K_{iB}' - K_B'}{K_{iB}} \leq \frac{k_2}{V/[E_t]} \leq \frac{K_C'}{K_C}\frac{K_{iB}' - K_B'}{K_{iB}}\frac{[EA_0^*]}{P^*_{max}} \quad (16)$$

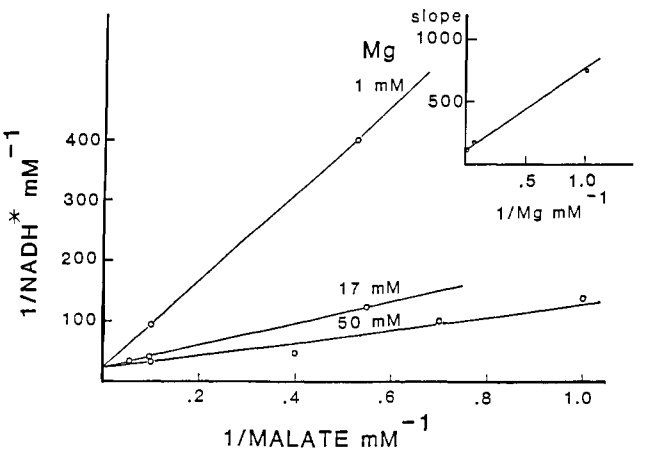

FIGURE 1: Isotope trapping of [^{14}C]NAD in the binary E·[^{14}C]NAD complex plotted in a double-reciprocal pattern of [^{14}C]NADH versus malate. A concentration of 0.091 mM (4.55 nmol) E·[^{14}C]NAD is used in each trapping experiment with the uncomplexed malate concentration varied from 1 to 10 mM and the uncomplexed Mg^{2+} concentrations fixed at levels at 1, 17, and 50 mM. (The line at 1 mM Mg^{2+} was based on three points at malate concentrations of 1, 2, and 10 mM. The point at 1 mM Mg^{2+} and 1 mM malate is not shown for clarity since it is off scale. The amount of [^{14}C]NADH trapped in this case is 0.00125 mM.) The experimental details are described under Materials and Methods. A replot of slope versus the reciprocal of the uncomplexed Mg^{2+} concentration is shown in the inset.

Table I: Summary of Kinetic Constants from Isotope Partitioning

parameter	
E·NAD* Trapping	
P^*_{max} (NADH*) (mM)	0.048 ± 0.003
K'_{malate} (mM)	5.4 ± 1.5
K'_{Mg} (mM)	0
K'_{iMg} (mM)	5.6 ± 2.0
E·Mg·NAD* Trapping	
P^*_{max} (NADH*) (mM)	0.051 ± 0.007
K'_{malate} (mM)	1.4 ± 0.1
E·Mg·Malate* Trapping	
P^*_{max} (alanine*) (mM)	0.045 ± 0.001
K'_{NAD} (μM)	0.70 ± 0.01

constant for B from EAB. The upper and lower limits are observed under the same condition as described above for k_9.

RESULTS

Two binary enzyme–substrate complexes (E·NAD; E·malate) and three ternary enzyme–substrate complexes (E·NAD·Mg; E·Mg·malate; E·NAD·malate) were used for isotope partitioning experiments, and each will be discussed below.

E·[^{14}C]NAD. A double-reciprocal plot of the amount of [^{14}C]NADH produced from E·[^{14}C]NAD vs the concentration of malate in the chase at different fixed levels of Mg^{2+} in the chase is shown in Figure 1. The three lines obtained at three different Mg^{2+} concentrations intersect on the ordinate, suggesting that K_B' is equal to zero. Under conditions where malate is saturating, the amount of [^{14}C]NADH trapped from E·[^{14}C]NAD is independent of the Mg^{2+} concentration. The kinetic constants obtained from a fit of eq 6 to the data in Figure 1 are shown in Table I. Under conditions where malate and Mg^{2+} are saturating, the maximum amount of [^{14}C]NAD trapped (P^*_{max}) is 0.048 ± 0.030 mM. The kinetic constants for trapping are K'_{malate} = 5.40 ± 1.50 mM and K'_{iMg} = 5.60 ± 2.00 mM.

E·NAD·Mg. As a check of the results obtained above, the isotope trapping experiment from E·NAD·Mg was carried out under the similar conditions, but starting with the E·NAD·Mg

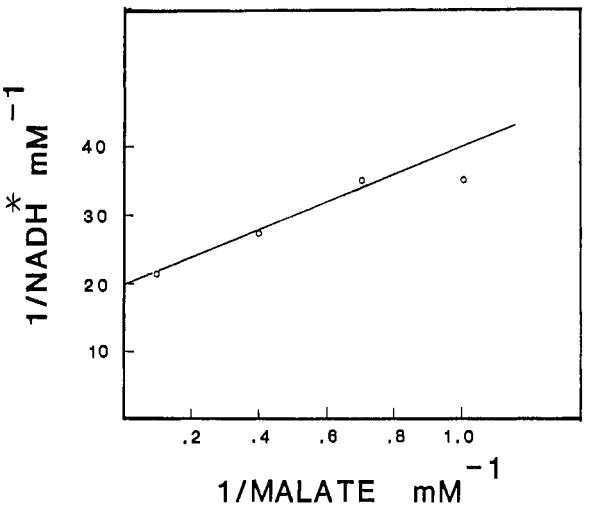

FIGURE 2: Isotope trapping of [^{14}C]NAD in the ternary E·[^{14}C]-NAD·Mg complex as shown in a double-reciprocal plot of [^{14}C]NADH versus malate. A concentration of 0.091 mM E·[^{14}C]NAD·Mg (corrected for the rapid equilibrium addition of Mg^{2+} in the chase solution as described under Results) is used in each trapping experiment. The amount of the uncomplexed malate was varied from 1 to 10 mM.

complex in the pulse and varying malate in the chase. For the conditions used for the pulse solution, E·[^{14}C]NAD is 0.022 mM and E·[^{14}C]NAD·Mg is 0.069 mM, and both can potentially give trapping as [^{14}C]NADH. In the chase, Mg^{2+} was included at 100 mM. Rewriting eq 8, setting K_B' equal to zero, gives eq 17, where $K'_{1\,Mg}$ = 5.6 mM and $K_{iB}'/[B]$

$$\frac{[EA^*]}{P^*} = \frac{[EA^*]}{P^*_{max}}\left[1 + \frac{K_C'}{[C]}\left(1 + \frac{K_{iB}'}{[B]}\right)\right] \quad (17)$$

equals 0.056, which is negligible. These conditions are equivalent to starting with 0.091 mM E·[^{14}C]NAD·Mg for the trapping experiment. Since the concentration of Mg^{2+} is high in these experiments, the AGMP-1 column chromatography could not be used to isolate NADH, and HPLC with a C_{18} reverse-phase preparative column was used. Data obtained as discussed above for these trapping experiments are plotted in double-reciprocal form as 1/[[^{14}C]NADH] vs 1/[malate] and shown in Figure 2. The P^*_{max} obtained is 0.05 mM, and the apparent K_i for malate is 1.4 ± 0.1 mM, Table I.

E·Malate. The pulse solution containing 10 mM EDTA and 0.06 mM E·[^{14}C]malate was added to a rapidly stirring chase solution that contained 0.5 mM uncomplexed NAD (100-fold higher than the K_m for NAD of 0.005 mM) and 50 mM uncomplexed Mg^{2+}. After 5 s, the reaction was quenched by increasing the pH above 12.5 with 10 N KOH, followed by back-titration to pH 9.0. No reactivation of enzyme was observed. The pyruvate was then converted to alanine and isolated as described under Materials and Methods. The amount of [^{14}C]alanine trapped from the E·[^{14}C]malate complex was identical in both experimental and control experiments.

E·Mg·Malate. These experiments were carried out the same as those for E·malate. The pulse solution contained 0.0067 mM E·[^{14}C]malate and 0.0843 mM E·Mg·[^{14}C]malate. Only the latter could potentially give trapping as [^{14}C]pyruvate, since E·[^{14}C]malate is a nonproductive complex. The resulting [^{14}C]pyruvate was converted to [^{14}C]alanine as described above. Data obtained were plotted (not shown) in double-reciprocal form, and the kinetic parameters were obtained by fitting eq 5 to the data. The P^*_{max} is 0.045 ± 0.001 mM, while

Scheme I[a]

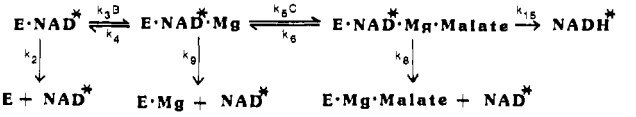

[a] B = Mg; C = malate.

K'_{NAD} is 0.70 ± 0.01 μM, Table I.

E·NAD·Malate. These experiments were carried out with [^{14}C]NAD in the E·[^{14}C]NAD·malate complex. The pulse solution contained 0.0145 mM E·[^{14}C]NAD and 0.083 mM E·[^{14}C]NAD·malate with 10 mM EDTA included to avoid turnover of malic enzyme as a result of trace amounts of Mg^{2+} contamination. The experiments were performed identically with the E·[^{14}C]NAD·Mg trapping experiments. However, the resulting [^{14}C]NADH is consistently 6-fold higher than the total amount of malic enzyme present. These data indicated that the enzyme in the pulse solution had turned over before it was injected into the chase solution. The malic enzyme used contained (0.2% or less) contamination by malate dehydrogenase. During the 10-min incubation time, 0.1% contamination of malate dehydrogenase (0.011 unit) could generate as much as 2.2 mM [^{14}C]NADH. Thus, the E·NAD·malate trapping experiments could not be carried out.

DISCUSSION

Isotope partitioning studies using Mg^{2+} as the divalent metal for NAD–malic enzyme suggest a steady-state random mechanism in the direction of oxidative decarboxylation of L-malate since trapping was obtained from both E·[^{14}C]-NAD·Mg and E·Mg[^{14}C]malate. These results are consistent with previous results from initial velocity studies (Park et al., 1984), protection against inactivation by DTNB (Kiick et al., 1984), and deuterium isotope effects (Kiick et al., 1986). The isotope partitioning data, when combined with the results of pH studies and deuterium isotope effects, provide a more quantitative description of the kinetic mechanism of the *Ascaris suum* NAD–malic enzyme. Each of the isotope partitioning experiments will be discussed in detail prior to summarizing the data.

(1) Isotope Partitioning Studies Beginning with the E·NAD Complex. Isotope partitioning studies as a quantitative probe of a terreactant enzyme mechanism were first used by Meek et al. (1982) to study glutamine synthetase. The mechanism used by Meek et al. (1982) and to interpret data obtained in these studies is shown in eq 7. As can be seen, A* may dissociate from any of three transitory enzyme complexes or be transformed to P*. In the case of glutamine synthetase, other information suggested an ordered reaction mechanism, thus simplifying the derivation of the isotope partitioning rate equation since k_8 and k_9 in eq 7 are equal to zero. However, the NAD–malic enzyme by all indications has a random mechanism, and k_9 and k_8 are not equal to zero. Previous results from initial velocity studies (Park et al., 1984) indicate that under conditions where NAD is saturating the mechanism is ordered and adheres to Scheme I, where E·A*, B, and C, are E·[^{14}C]NAD, Mg, and malate, respectively. Unlike a bireactant enzyme reaction, when one begins with a binary complex, there are two reactants that can be varied in the chase solution in the case of a terreactant enzyme reaction. As a result, the experiment is carried out varying one reactant at several different fixed levels of the second, and one obtains an isotope partitioning pattern. A double-reciprocal plot of [^{14}C]NADH (produced from E·[^{14}C]NAD) vs malate at several different fixed levels of Mg^{2+} gives three lines that

Table II: Dissociation Constants for Enzyme-Reactant Complexes

enzyme form[a]	K_I	values ± SE
EA	K_{iA}	0.080 ± 0.001 mM[b]
EAB	K_{IA}	0.078 ± 0.004 mM[d]
EBC	K_{IC}	1.6 ± 0.3 mM[c]
EAB	K_{IB}	29.3 ± 1.3 mM[c]
EB	K_{iB}	14.0 ± 1.0 mM[c]
EAC	K_{IC}'	35.0 ± 0.8 mM[c]
EAC	K_{IA}'	0.14 ± 0.03 mM[e]
EC	K_{iC}	20.0 ± 2.0 mM[c]
EABC	K_C	1.2 ± 0.1 mM[b]
EABC	K_A	0.005 ± 0.001 mM[b]

[a] A = NAD; B = Mg^{2+}; C = malate. [b] The results from initial velocity studies by Park et al. (1984). [c] The results from protection against inactivation titration by DTNB studies by Kiick et al. (1984). [d] Determined by the equation $K_{IA} = K_{iA}K_{IB}/K_{iB}$. [e] Determined by the equation $K_{IA}' = K_{iA}K_{IC}'/K_{iC}$.

intersect on the ordinate. These results indicate that the K_B' term equal to k_2/k_3 is zero. As a result, the on-rate for Mg^{2+} to form E·NAD·Mg (k_3 in Scheme I) is much greater than the off-rate of NAD from the E·NAD complex (k_2 in Scheme I). This information combined with a value of $k_2/(V/[E_t])$ near unity suggests that Mg^{2+} adds in rapid equilibrium prior to malate, consistent with results from initial velocity studies (Park et al., 1984).

From P^*_{max}, the ratio of the off-rate of NAD from the quaternary E·NAD·Mg·malate complex (k_8 in Scheme I) to the catalytic rate (k_{15} in Scheme I) is 0.90 + 0.06. The rate constant k_{15} includes all the steps from the E·NAD·Mg·malate quaternary complex to the release of the first product, probably CO_2. Deuterium isotope effect and double inhibition studies (Kiick et al., 1986) suggested that the off-rate of NAD from E·NAD·Mg·malate (k_8) is equal to the off-rate of NADH from the E·NADH complex ($k_{off\,NADH}$) so that the release of NADH and the catalytic steps are both partially rate limiting. With $k_8/k_{off\,NADH}$ equal to 1 and k_8/k_{15} equal to 0.9, the off-rate of NADH from E·NADH ($k_{off\,NADH}$) must also be approximately equal to k_{15}.

The specific activity of the malic enzyme preparations used in these studies was 34 units/mg. On the basis of a subunit M_r of 65 000, the enzyme turnover number ($V/[E_t]$) is 37 s^{-1}. Since $V/[E_t]$ is only limited by the off-rate of NADH ($k_{off\,NADH}$) and the catalytic rate (k_{15}) (Kiick et al., 1986) and these two rate constants are equal, values of k_{15} and the off-rate for NADH from E·NADH ($k_{off\,NADH}$) are calculated with eq 18. This gives a catalytic rate (k_{15}) of 78 ± 5 s^{-1}. The

$$\frac{V}{[E_t]} = \frac{1}{1/k_{15} + 1/k_{off\,NADH}} \qquad (18)$$

off-rates of NADH from E·NADH ($k_{off\,NADH}$) and NAD from E·NAD·Mg·malate (k_8) are identical and equal to 70 ± 6 s^{-1}.

Release of NAD from the E·NAD·Mg complex (k_9 in Scheme I) is calculated from eq 14 to be between the limits 5.0 ± 1.0 and 9.0 ± 2.0 compared to enzyme turnover ($V/[E_t]$), and k_9 is thus calculated to be 2.2 ± 0.6 to 4.0 ± 1.0 times greater than k_{15}. The release of NAD from E·NAD (k_2 in Scheme I) is calculated from eq 16 to be between 2.0 ± 1.0 and 4.0 ± 2.0 compared to $V/[E_t]$, giving values for k_2/k_{15} of 0.8 ± 0.4 to 2.0 ± 1.0. The value of k_9 is (2.5 ± 0.9)-fold greater than k_2, and thus, the presence of Mg^{2+} in the active site may slightly decrease the affinity for NAD. However, the dissociation constants of NAD in the presence and absence of Mg^{2+} ($K_{i\,NAD}$ and $K_{I\,NAD}$) are identical as shown in Table II, suggesting that the binding of Mg^{2+} does not affect the affinity of NAD and that k_2 and k_9 should be identical as they are within experimental error. From the above data, the

Scheme II[a]

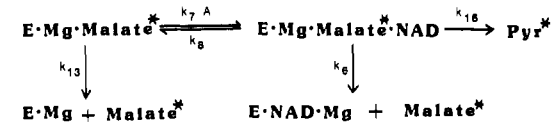

[a] A = NAD.

off-rate of NAD from E·NAD·Mg (k_9) is (2.0 ± 1.0)- to (5.0 ± 1.0)-fold greater than the off-rate for NAD from the central complex (k_8), and thus, the presence of malate in the active site slightly decreases the off-rate of NAD. A more accurate value for the latter is obtained from the E·NAD·Mg experiment, and this will be discussed below.

(2) *Isotope Partitioning Studies Beginning with the E·NAD·Mg Complex.* The value of P^*_{max} from Figure 2 allows calculation of k_8/k_{15}, giving a value approximately identical with the value obtained from trapping experiments beginning with E·NAD. However, the value of K'_{malate} from this experiment is 1.4 mM, lower than the value of 5.4 mM obtained from the E·NAD trapping experiment. The value of 1.4 mM should be the more accurate of the two as indicated by the relative standard errors. In addition, the value of 1.4 mM for K'_{malate} was obtained from an experiment in which only malate was varied while the higher value was obtained from a pattern in which two reactants were varied requiring two extrapolations. For the kind of experiments carried out, the two values are in reasonable agreement. The value of 1.4 mM for K_{malate} allows calculation of limits of 1.2 ± 0.3 to 2.3 ± 0.6 for $k_9/(V/[E_t])$, giving limits of 0.6 ± 0.2 to 1.1 ± 0.3 for k_9/k_{15}. Thus, the off-rate of NAD from E·NAD·Mg (k_9) is about equal to the off-rate of NAD from the central complex (k_8), suggesting that the presence of malate does not affect the affinity of NAD significantly. Results are consistent with the essential identity between the dissociation constants for NAD ($K_{i\,NAD}$ and $K_{I\,NAD}$) in the presence and absence of malate, Table II.

(3) *Isotope Partitioning Beginning with the E·Malate Complex.* No [^{14}C]malate over control was obtained in the E·malate binary complex trapping experiment. Previous results from initial velocity studies (Park et al., 1984) have suggested that both E·malate and E·NAD·malate are nonproductive and dead-end, and as a result, one expects no trapping from these complexes. Data are consistent with either an insufficiently high Mg^{2+} concentration to trap [^{14}C]malate from E·malate or a nonproductive E·malate complex. The amount of $MgSO_4$ able to be added to the chase once correction was made for the metal–substrate chelate complexes is limited, and the highest amount possible was 50 mM.

(4) *Isotope Partitioning Beginning with the E·Mg·Malate Complex.* Two radiolabeled enzyme–substrate complexes (E·[^{14}C]malate and E·Mg·[^{14}C]malate) were present in the pulse solution in these experiments. However, as shown above, at 50 mM Mg^{2+}, no trapping could be detected. Thus, all of the [^{14}C]pyruvate trapped in these experiments must be from the E·Mg·[^{14}C]malate complex. The calculated ratio of the off-rate of malate from the E·NAD·Mg·malate complex (k_6 in Scheme II) to k_{15}, the rate of labeled product formation, is 0.9 ± 0.1, identical with k_8/k_{15} obtained from [^{14}C]NAD trapping. Kiick et al. (1986) obtained identical isotope effects on V/K_{NAD} and V/K_{malate} suggesting that the off-rates of NAD and malate from the quaternary E·NAD·Mg·malate complex are identical and in excellent agreement with the results of trapping experiments. The ratio of the off-rate of malate from the E·Mg·malate complex (k_{13} in Scheme II) to $V/[E_t]$ is within the limits of 0.1–0.3. Using a value $k_{15}/(V/[E_t])$ =

Scheme III

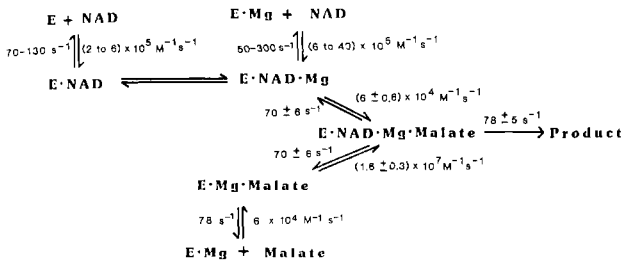

2.1 (from above), k_{13}/k_{15} is calculated as 0.05–0.15. These results indicate that k_{13} is less than k_6. In this respect, two things must be considered. First, to determine K'_{NAD}, the uncomplexed NAD concentration was varied over a very low range (1–5 μM), and the final concentration of uncomplexed NAD is directly related to the concentration of $MgSO_4$ included and the accuracy to which the stability constant of the chelate complex Mg·NAD is known.[2] Thus, the value of K'_{NAD} can only be considered an estimate. Second, the dissociation constants for malate in the presence of Mg^{2+} and in the presence (K_C) and absence of NAD (K_{IC}) shown in Table II (Kiick et al., 1984) are for all intents and purposes identical. An accurate value for k_{13}/k_{15} cannot be determined from K'_{NAD}. On the basis of the equality of K_C and K_{IC}, we will assume for the present analysis that the ratio is 1.

Summary of Isotope Partitioning Data. The present data are summarized in Scheme III. Since the values of k_6 (70 ± 6 s^{-1}), k_8 (70 ± 6 s^{-1}), and k_{15} (78 ± 5 s^{-1}) have been determined, all of the values required for determining estimates of the absolute values of the off-rates from enzyme–substrate complexes are available. Thus, one can calculate values for k_9 and k_{13} using eq 26 and a value for k_2 using eq 28 [except in the calculation of k_{13}, eq 26 needs to be modified where k_9 is replaced by k_{13} and $k_6/(k_6 + k_8 + k_{15})$ is replaced by $k_8/(k_6 + k_8 + k_{15})$; EA* is replaced by EBC*; K_C' and K_C are replaced by K_A' and K_A, respectively]. Absolute values of k_9 are estimated as 45 ± 11 to 85 ± 22 s^{-1} from E·NAD trapping and 170 ± 40 to 320 ± 90 s^{-1} from E·NAD·Mg trapping for an overall range of about 50–300 s^{-1}. Absolute values of k_2 are estimated as 67 ± 30 to 130 ± 60 s^{-1} for an overall range of about 70–130 s^{-1}. The absolute value of k_{13} is probably 70 s^{-1} as discussed above. With the values of K_iNAD (for E·NAD) and K_INAD (for E·NAD·Mg) shown in Table II, the association rates of NAD to form E·NAD (k_1 in Scheme III) and E·NAD·Mg (k_{10} in Scheme III) complexes can also be calculated with k_1 estimated as (2–16) × 10^5 M^{-1} s^{-1}, and k_{10} is estimated as (6–40) × 10^5 M^{-1} s^{-1}. With the value of $K_{I\,malate}$ shown in Table II, the association rate for malate to form E·Mg·malate (k_{14} in Scheme III) can also be calculated as 6 × 10^4 M^{-1} s^{-1}. The K_m values for NAD and malate are equal to their K_d value since the deuterium isotope effects on V, V/K_{malate}, and V/K_{NAD} are equal (Klinman & Matthews, 1985). Thus, the on-rate of NAD to E·Mg·malate and malate to E·NAD·Mg can also be calculated as (1.6 ± 0.3) × 10^7 M^{-1} s^{-1} (k_7) and (6.0 ± 0.6) × 10^4 M^{-1} s^{-1} (k_5), respectively. The calculated values for substrate addition rates are much lower than the diffusion limit (except perhaps in the case of NAD binding to E·Mg·malate) of 10^8–10^9 M^{-1} s^{-1}, suggesting that there are additional steps (perhaps conformational changes) involved in the addition of substrate.

[2] The range of desired concentrations for uncomplexed NAD is 4 orders of magnitude lower than the Mg·NAD stability constant of 19.5 mM, while the uncomplexed malate concentration (1–50 mM) varied in the vicinity of the Mg·malate stability constant of 25.1 mM.

The initial velocity studies carried out by Landsperger et al. (1978) indicate that the $V_{max}/[E_t]$ in the direction of oxidative decarboxylation is 30-fold higher than the $V_{max}/[E_t]$ in the direction of the reductive carboxylation of pyruvate. Thus, the turnover number ($V_r/[E_t]$) in the reverse direction can be calculated as 1.2 s^{-1}. Since both NAD and malate dissociate at a rate faster than $V_r/[E_t]$, it is suggested that the rates of release of both NAD and malate will not be rate-limiting steps in the reverse direction.

Previous Isotope Partitioning Studies with Mn^{2+}. Isotope partitioning using Mn^{2+} has been carried out previously for the NAD–malic enzyme (Landsperger et al., 1978). However, in the earlier study several things were not considered. Studies were carried out only with the terreactant complexes (E·Mn·[^{14}C]NAD and E·Mn·[^{14}C]malate), and under the conditions used, the pulse solution also contained binary complexes (E·[^{14}C]NAD and E·[^{14}C]malate). Since E·malate has been identified as nonproductive, trapping from E·Mn·[^{14}C]malate should only have a contribution from the ternary complex. However, determination of the relative rates using isotope partitioning techniques requires an accurate concentration of the initial enzyme–substrate complex present in the pulse. Since the dissociation constants are not known with Mn^{2+} and the concentration of the ternary complex is overestimated as a result of the presence of binary complex, values of k_6/k_{15} and k_8/k_{15} are at least underestimated and still cannot be quantitated. Values of K', the concentration of the substrate varied in the chase solution to give half the maximum amount of trapping, should present less problems. The value of K'_{NAD} should be accurate since E·malate does not give trapping and K'_{malate} will reflect binding to both E·Mn·NAD and E·NAD, but the latter with malate bound is nonproductive since Mn^{2+} in the chase is not high enough to give sufficient E·NAD·Mn·malate from the existing E·NAD. The value of K_{NAD} obtained by Landsperger et al. (1978) is 0.25 mM, which is 250-fold higher than the value obtained with Mg^{2+}. Data suggest that malate partitions toward product formation from the E·M^{2+}·malate complex in the presence of Mg^{2+} much more than in the presence of Mn^{2+}. The value of K'_{malate} obtained by Landsperger et al. (1978) is 4.6 mM, similar to the value obtained with Mg^{2+}.

Data of Landsperger et al. (1978) indicate that malate dissociates from the central complex 10-times faster than NAD but that both are bound more tightly in the ternary complexes. Recently, deuterium isotope effects on V/K_{NAD} and V/K_{malate} have been measured with Mn^{2+} as the divalent metal ion (unpublished data of S. R. Gavva in this laboratory). These data provide another estimate of the relative off-rate of NAD and malate from E·NAD·Mn·malate. Values of $^D(V/K_{malate})$ and $^D(V/K_{NAD})$ are 2.2 and 1.6, respectively, indicating that the off-rate of malate is twice as fast as that of NAD from E·NAD·Mn^{2+}·malate. Thus, although the previous data can be used qualitatively and are in agreement with the present study, the studies cannot be compared quantitatively.

ACKNOWLEDGMENTS

We thank Rita Huber for typing the manuscript.

REFERENCES

Allen, B. L., & Harris, B. G. (1981) *Mol. Biochem. Parasitol. 2*, 367.

Atkins, J. F., Lewis, J. B., Anderson, C. W., & Gesteland, R. F. (1975) *J. Biol. Chem. 250*, 5688.

Bradford, M. (1976) *Anal. Biochem. 72*, 248.

Cleland, W. W. (1975) *Biochemistry 14*, 3220.

Cleland, W. W. (1979) *Methods Enzymol. 63*, 103.

Cook, P. F., Blanchard, J. S., & Cleland, W. W. (1980) *Biochemistry 19*, 4853.
Kiick, D. M., Allen, B. L., Rao, J. G. S., Harris, B. G., & Cook, P. F. (1984) *Biochemistry 23*, 5454.
Kiick, D. M., Harris, B. G., & Cook, P. F. (1986) *Biochemistry 25*, 227.
Klinman, J. P., & Matthews, R. G. (1985) *J. Am. Chem. Soc. 107*, 1058.
Landsperger, W. J., Fodge, D. W., & Harris, B. G. (1978) *J. Biol. Chem. 253*, 1868.
Martell, A. E., & Smith, R. M. (1979) *Critical Stability Constants*, Vol. 3, Plenum, New York.
Meek, T. D., Johnson, K. A., & Villafranca, J. J. (1982) *Biochemistry 21*, 2158.
Miksic, J. R., & Brown, P. R. (1977) *J. Chromatogr. 142*, 64.
O'Farrel, P. H. (1975) *J. Biol. Chem. 250*, 4007.
Park, S.-H., Kiick, D. M., Harris, B. G., & Cook, P. F. (1984) *Biochemistry 23*, 5446.
Rose, I. A. (1980) *Methods Enzymol. 64*, 47.
Rose, J. A., O'Connell, E. L., Litwin, S., & Bar-Tana, J. (1974) *J. Biol. Chem. 249*, 5163.
Viola, R. E., Cook, P. F., & Cleland, W. W. (1979) *Anal. Biochem. 96*, 334.

Enzymatically Active Angiogenin/Ribonuclease A Hybrids Formed by Peptide Interchange†

J. Wade Harper, David S. Auld, James F. Riordan, and Bert L. Vallee*

Center for Biochemical and Biophysical Sciences and Medicine and Department of Pathology, Harvard Medical School and Brigham and Women's Hospital, Boston, Massachusetts 02115

Received July 17, 1987; Revised Manuscript Received September 11, 1987

ABSTRACT: The primary structures of the blood vessel inducing protein human angiogenin and human pancreatic ribonuclease (RNase) are 35% identical. Angiogenin catalyzes the limited cleavage of ribosomal RNA (18 and 28 S), yielding a characteristic pattern of polynucleotide products, but shows no significant activity toward conventional pancreatic RNase substrates [Shapiro, R., Riordan, J. F., & Vallee, B. L. (1986) *Biochemistry 25*, 3527–3532]. Angiogenin/RNase hybrid enzymes—wherein particular regions of primary structure in RNase are replaced by the corresponding segments of angiogenin—serve to explore the structural features underlying angiogenin's characteristic activities. Herein we show that synthetic angiogenin peptides, Ang(1–21) and Ang(108–123), form noncovalent complexes with inactive fragments of bovine RNase A—RNase(21–124) (i.e., S-protein) and RNase(1–118), respectively—with regeneration of activity toward conventional RNase substrates. Maximal activities for the Ang(1–21)/S-protein complex (K_d = 1.0 μM) are 52%, 45%, and 15% toward cytidine cyclic 2′,3′-phosphate, cytidylyl(3′→5′)adenosine, and yeast RNA, respectively. In contrast, activities of the RNase(1–118)/Ang(108–123) hybrid (K_d = 25 μM) are 1–2 orders of magnitude lower toward cyclic nucleotides and dinucleoside phosphates. However, substitution of phenylalanine for Leu-115 in Ang(108–123) increases activity up to 100-fold. Both His-13 and His-114 in the angiogenin peptides are required for activity since their substitution by alanine yields inactive complexes. Importantly, the pattern of polynucleotide products formed during cleavage of ribosomal RNA by the Ang(1–21)/S-protein hybrid shows a striking resemblance to that formed by angiogenin, demonstrating that the hybrid retains features of both angiogenin and RNase A. In contrast, neither RNase(1–118)/Ang(108–123) nor S-peptide/S-protein complexes produce this cleavage pattern. Thus, the data point to an important role for the N-terminal region of angiogenin in conferring substrate selectivity.

Human angiogenin is a blood vessel inducing protein whose primary structure is 35% identical with that of human pancreatic ribonuclease (RNase)[1] (Fett et al., 1985; Strydom et al., 1985; Kurachi et al., 1985). Preliminary energy minimization and molecular modeling studies indicate that the polypeptide backbones of the two proteins are readily superimposable within the regions of their α-helical and β-sheet structures (Palmer et al., 1986). The three active site residues identified for RNase—His-12, Lys-41, and His-119—have direct counterparts in angiogenin, and indeed, angiogenin has been found to exhibit ribonucleolytic activity. This activity differs markedly, however, from that of pancreatic RNase: it

† This work was supported by funds from Monsanto Co. under agreements with Harvard University. J.W.H. was supported by National Research Service Award HL-07075 from the National Heart, Lung, and Blood Institute.

* Address correspondence to this author at the Center for Biochemical and Biophysical Sciences and Medicine, Harvard Medical School, Boston, MA 02115.

[1] Abbreviations: RNase, pancreatic ribonuclease; RNase A, bovine pancreatic ribonuclease A; C>p, cytidine cyclic 2′,3′-phosphate; U>p, uridine cyclic 2′,3′-phosphate; UpN and CpN, uridine and cytidine 3′,5′-dinucleoside phosphates where N represents adenine or guanine; K_d, apparent dissociation constant for the peptide/protein complex; Mes, 2-(*N*-morpholino)ethanesulfonic acid; C18, octadecylsilane; HPLC, high-performance liquid chromatography; Tris, tris(hydroxymethyl)-aminomethane; TFA, trifluoroacetic acid; Boc, *tert*-butyloxycarbonyl; Tos, *p*-toluenesulfonyl; Bzl, benzyl; Br-Z, (2-bromobenzyl)oxycarbonyl; Cl-Z, (2-chlorobenzyl)oxycarbonyl; DCC, *N*,*N*′-dicyclohexylcarbodiimide; Hepes, 4-(2-hydroxyethyl)-1-piperazineethanesulfonic acid; EDTA, ethylenediaminetetraacetic acid.

0006-2960/88/0427-0219$01.50/0